

Contrail formation and impacts on aerosol properties in aircraft plumes: Effects of fuel sulfur content

Fangqun Yu and Richard P. Turco*

Department of Atmospheric Sciences, University of California, Los Angeles

*Institute of Geophysics and Planetary Physics, UCLA

Abstract. The formation and evolution of fine particles and ice contrails in an aircraft exhaust plume containing varying amounts of fuel sulfur have been simulated using an advanced aerosol microphysics model. The "core" sulfate and soot particles are tracked during the contrail formation and dissipation phases. When ion electrostatic effects are incorporated into the microphysics, sulfuric acid vapor emitted by high-sulfur-content fuels generates water-soluble particles that are large enough to be activated into contrails, improving the agreement between simulations and measurements. Our results also suggest that ice crystals formed in contrails efficiently scavenge vapors and particles, creating a sulfate aerosol accumulation mode that may contribute to cloud CCN/IN. The size distributions of aerosols produced both in the presence and absence of contrails agree reasonably well with the two characteristic types observed in the plumes of commercial aircraft.

Introduction

Contrails that form behind aircraft at cruise altitudes are of particular relevance to the impact of aviation on atmospheric chemistry and climate (Schumann, 1994; WMO, 1995). The thermodynamic conditions for contrail formation are well understood (Appleman, 1953). However, the mechanisms of particle formation and evolution, their chemical composition, size distribution, and hydration properties, the fraction of such particles active as cloud condensation nuclei (CCN) or ice nuclei (IN), and the effects of soot and sulfur on the optical and microphysical properties of the contrails and associated high-altitude clouds remain largely unresolved. This lack of understanding contributes to the uncertainty in evaluating the atmospheric impacts of aviation (Friedl, 1997).

Sampling of the total concentration, size distribution, and solubility of particles in the near-field of commercial aircraft (roughly, up to ~ 10 km behind flights operating at ~ 10 km altitude) reveals two distinct particle size spectra (Hagen et al., 1996); type I exhibits a Junge-like size distribution for diameters between $0.01 \mu\text{m}$ to $0.2 \mu\text{m}$, while type II is characterized by a Junge size distribution at small sizes ($0.01 \mu\text{m}$ to $0.04 \mu\text{m}$), and a larger-particle mode (peak between 0.1 and $0.2 \mu\text{m}$). Both types are also characterized by very high concentrations of fine particles, suggesting nucleation in the plume. Hagen et al. (1996) noted that significant numbers of exhaust particles (for example, those with dry diameters ~ 33 nm) have a high soluble mass fraction. Schumann et al. (1996) found significant differences in particle concentrations and contrail optical properties in side-by-side plumes from the same aircraft whose engines burned fuels with different fuel sulfur contents (FSC's) of 170 and 5500 ppm. These measurements demonstrate that fuel sulfur emissions have the capacity to modify significantly the character of plume aerosols and contrails.

Various model simulations of aircraft plume aerosols (Zhao and Turco, 1995; Kärcher et al., 1995; Brown et al., 1996a; Yu and Turco, 1997) and contrails (Brown et al., 1996a, 1997; Kärcher et al., 1995) suggest that volatile droplets can be formed by the prompt nucleation of H_2SO_4 and H_2O vapors, and that these particles may subsequently affect contrail properties. Kärcher (1996) considered the uptake of HNO_3 by liquid acid droplets, and concluded that some might be

converted into concentrated $\text{HNO}_3/\text{H}_2\text{O}$ solutions (containing small amounts of H_2SO_4) if the ambient temperature were low enough. Brown et al. (1996a) found that, in their simulations, sulfuric acid particles did not grow large enough to act as CCN. Kärcher (1996) predicted small numbers of volatile CCN, which did not greatly affect contrail properties. Thus, the qualitative differences in contrail properties seen when different FSC fuels are burned has been attributed to the fraction of soot particles activated as CCN, which is presumed to be related to FSC (Schumann et al., 1996; Gierens and Schumann, 1996; Brown et al., 1997). Comparing model simulations with in-situ measurements, Yu and Turco (1997) concluded that ions produced by chemiionization reactions within the engine combustors can accelerate the growth of volatile particles, and generate the largest aerosols seen in aircraft plumes, providing a new potential source of CCN.

In this work, the properties of plume aerosols (size distribution and composition), and the effects of contrail formation on these properties, are simulated using a comprehensive model of multi-component size-resolved aerosols, which distinguishes between water and ice particles, and tracks electrical charge. Model results are compared with measurements and implications for plume microphysics are discussed.

Plume Microphysics

Until the onset of contrail formation, the sizes of the volatile particles in an aircraft plume depend on the concentration of H_2SO_4 vapor, which is a function of the fuel sulfur content (FSC) and fraction emitted in the form of acidic compounds, S_c , the accommodation coefficient for H_2SO_4 vapor condensation, the coagulation kernel for nanometer size particles, and the influence of electrical and dynamical processes (Yu and Turco, 1997). As the exhaust gases mix isobarically with cool ambient air, water droplets can appear when the mixture achieves saturation with respect to water (Appleman, 1953). The number of droplets formed, and hence the properties of the resulting contrail, depends on the availability of CCN, which is a function of the size distribution of the volatile aerosols (owing to the Köhler effect), and of the fraction of soot particles that have been pre-activated (since these will exhibit hygroscopic behavior). Following activation, a subset of the water droplets will freeze and continue to grow at the expense of the remaining liquid droplets (as the relative humidity approaches the saturation level over ice), since the $\text{RH}_{\text{ice}} > \text{RH}_{\text{water}}$ in the same air parcel. Once the humidity in the plume falls below the ice saturation point ($\text{RH}_{\text{ice}} < 100\%$), the ice evaporates and the contrail dissipates, leaving behind a residue of processed "core" aerosols. In this study, the possible uptake of HNO_3 by plume aerosols (Kärcher, 1996) is not considered.

Ionization Effects: Chemiionization in hydrocarbon flames is known to generate high concentrations of ions (up to $10^{11}/\text{cm}^3$; Calcote 1962; Keil et al., 1984). Hence, it is reasonable to expect that ions and charged particles exist in substantial numbers in aircraft exhaust (Frenzel and Arnold, 1994; Yu and Turco, 1997). Charge-assisted growth associated with rapid molecular clustering onto ions (intrinsic ion nucleation), as well as electrically enhanced condensation and coagulation, can cause fine aerosols to grow much more rapidly in relation to neutral molecule/particle processes. An effective increase in the coagulation kernel due to electrification can be especially important in a system where particle evolution is controlled by the competing effects of coagulation and dilution (Turco and Yu, 1997). In the simulations discussed below, the effects of ionization on particle growth are critical in determining the number of volatile

aerosols large enough to act as CCN for contrail formation (refer to Yu and Turco, 1997).

Freezing of Water Droplets: Owing to the low temperatures at which contrails form in the present case (< -35 °C), homogeneous freezing is the dominant process leading to ice (DeMott, 1990). Accordingly, heterogeneous freezing induced by soot cores embedded in liquid droplets (which may be important when $T > -34$ °C) is not considered here. The parameterized homogeneous freezing rate used in our calculations is extrapolated from experimental data (DeMott and Rogers, 1990).

Simulations

Aerosol Model Structure: Particles are discretized into 61 geometric size bins representing diameters from 0.55 nm to 2 μm , with particle volumes having a ratio of 1.5 between adjacent bins. A hybrid bin structure is adopted (Jacobson and Turco, 1995) with a fixed core component of either soot and/or sulfur acid. This approach allows the core components to be tracked accurately as particles are activated, grow, and evaporate rapidly, which is important in analyzing post-contrail particle properties. The water content of unactivated aerosols is determined by assuming instantaneous water vapor equilibrium within the plume environment (Jacobson et al., 1996), while the water content of activated droplets is determined by integrating the time-dependent net kinetic flux of water vapor to the particle surface.

Pure soot, sulfuric acid (H_2SO_4 and H_2O), and mixed (soot, H_2SO_4 and H_2O) particles comprise the three basic types of aerosol treated in the model. However, when ion effects are considered, the evolution of the charged and neutral populations of volatile acid particles are also explicitly followed. Further, if a contrail forms, we distinguish between liquid water and ice particles, and quantify their competition for water vapor (calculating the shift of water from the liquid to ice phase, as occurs in clouds). Coalescence of unactivated aerosols with water/ice particles is included. When a contrail particle evaporates in subsaturated air, its core aerosol is subsequently maintained in water vapor equilibrium with the environment. The semi-implicit algorithms used here to calculate condensation, coagulation and coalescence rates have been shown to be efficient, stable and mass conserving (e.g., Turco et al., 1979).

Flight Conditions and Emission Parameters: The particular plume configuration investigated in this work applies to a recent series of field measurements in the upper troposphere (Schumann et al., 1996). The ambient pressure, temperature (T_a), and relative humidity were 287 hpa, -55 °C and 40%, respectively. Here, we focus on the evolution of the plume aerosols and contrail generated by one engine burning high-sulfur-content (5500 ppm) fuel. The emission index and size distribution of the soot particles are, respectively, $EI_{\text{soot}} = 0.2$ g/kg, and a log-normal distribution with $\sigma = 1.5$ and a mean mass diameter of 60 nm; these choices provide the best fit to the measured concentrations of particles larger than 120 nm and larger than 18 nm in the plume from the engine burning low-sulfur-content fuel (these particles are considered to consist mainly of soot inasmuch as acid particles are unlikely to grow larger than 18 nm in the low sulfur plume; Yu and Turco, in prep.). A key parameter in this study is the fraction of fuel sulfur, S_c , oxidized to S(VI) (i.e., $\text{H}_2\text{SO}_4 + \text{SO}_3$) shortly after emission. Based on simulations with a combustion chemistry code, Brown et al. (1996b) concluded that S_c does not scale linearly with FSC (for example, they found $S_c \approx 1\%$ for FSC = 5500 ppm, and $S_c \approx 4\%$ for FSC = 170 ppm). In the present study, we chose $S_c = 1.5\%$ for the high-sulfur plume. An initial ion concentration of $10^8/\text{cm}^3$ was also assumed.

Results

Plume Thermodynamics: In Figure 1, the growth in the diameter of the exhaust plume has been interpolated from the observations of Schumann et al. (1996), and the plume temperature calculated using the corresponding dilution factor. The evolution of plume relative humidity with respect to pure liquid water (RH_{water}) and ice (RH_{ice}) is also illustrated. The liquid water saturation point is reached at about ~ 0.1 sec after emission, and the maximum supersaturation (over liquid water) reaches about 25%. Ice supersaturation, correspondingly,

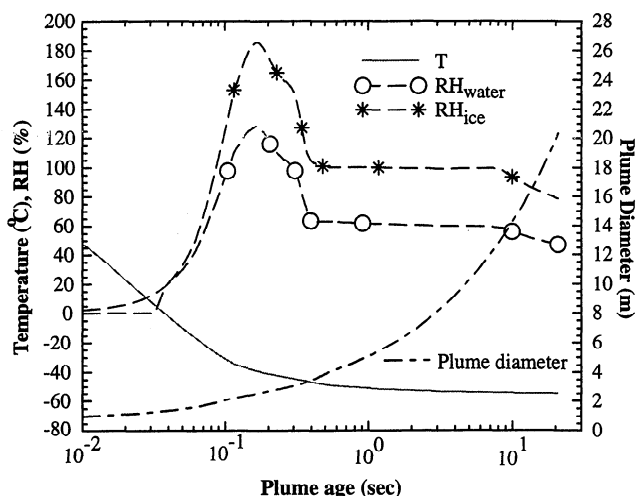


Figure 1. Time evolution of plume temperature, relative humidity with respect to liquid water and ice (RH_{water} , RH_{ice}), and plume diameter up to 21 sec into the wake.

reaches 85%. At such high supersaturations, it is likely that most of the emitted soot particles will be active as water condensation sites. For example, laboratory data show that soot particles with diameters > 80 nm behave like CCN for water supersaturations of 2% (DeMott, 1990). Thus, differences in the properties of contrails produced by different fuel sulfur contents would not seem to be directly attributable to differences in the fraction of activated soot particles. Water vapor supersaturation achieves its maximum value at ~ 0.16 sec, then falls off due to efficient condensation of water vapor onto activated aerosols. As these liquid particles begin to freeze at ~ 0.25 sec, the relative humidity decreases even more rapidly owing to the higher supersaturations that exist over the ice crystals, and the larger ice surface area. The ice mass increases steadily until the relative humidity stabilizes ($\text{RH} \approx \text{RH}_{\text{ice}} \approx 100\%$) by ~ 0.4 sec. Beyond that point, as plume dilution continues, the ice particles begin to evaporate, maintaining $\text{RH} \approx \text{RH}_{\text{ice}} \approx 100\%$. By about 8 sec after emission, most of the ice has evaporated and the contrail has dissipated. This simulated behavior is typical of both the high and low FSC wakes.

Note that our dynamically simplified analysis assumes uniform mixing across the plume cross section, representing "average" conditions within the wake. Accordingly, it is likely that visual observations of the contrail onset and dissipation will not coincide precisely with simulations owing to non-homogeneous effects.

Size Distribution Evolution: Figure 2 shows changes in the concentrations of particles in several different size ranges during contrail evolution in the high-sulfur (HS) wake. Almost all the soot particles ($\sim 90\%$) are activated as CCN, and subsequently freeze, while the rest remain as mixed aerosols (refer to the $d > 18$ nm liquid mixed particles in Fig. 2a). Even before the maximum water vapor supersaturation is achieved, significant numbers of sulfuric acid particles have grown larger than 18 nm aided by electrostatic effects (Fig. 2b). These large volatile particles have a sufficiently low Köhler barrier to be activated into growing water droplets (indicated as the $d > 120$ nm liquid acid particles in Fig. 2b). However, only about 10% of these activated acid droplets eventually freeze and continue to grow as ice crystals, while the remainder recede to their unactivated state. This occurs because the largest mixed particles (with soot cores) are activated and freeze sooner, and then effectively scavenge water vapor in the plume (including water that evaporates from liquid aerosols, making them less likely to freeze).

Based on these simulations, we expect that a contrail formed in an HS plume will initially have a greater optical depth compared with one formed in a low-sulfur (LS) plume (since fewer acid particles will have grown large enough to be activated in the latter case). This initial difference in optical depth would become less noticeable as the unfrozen activated acid droplets lost water to ice and shrank. Such general inferences from our calculations (Figure 2) are consistent with observations of HS and LS contrails (Schumann et al., 1996).

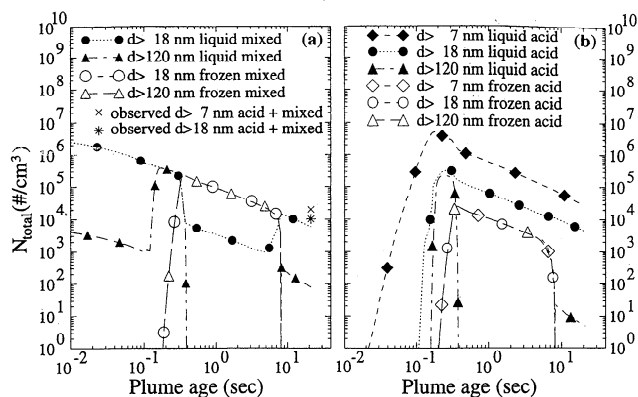


Figure 2. Evolution of the abundance of particles in several size ranges (as indicated) in a high-sulfur (HS) jet plume. The liquid and frozen species are treated as distinct types of aerosols. Panel (a) shows changes in the number of mixed (soot coated with acid) particles; and panel (b), pure sulfuric acid particles. The total particle concentrations in each size range include all states of electrical charge. Also indicated in panel (a) are observed total (acid + mixed) concentrations of particles with $d > 7 \text{ nm}$ and $d > 18 \text{ nm}$.

Following contrail evaporation, the concentration of particles having diameters greater than 18 nm is calculated to be $N_{d>18 \text{ nm}} \sim 10,000/\text{cm}^3$ at 21 sec , which agrees well with the observations of Schumann et al. (1996) for that time. The model also indicates that nearly half of these particles would be fully volatile (sulfuric acid and water). The concentration of such particles that are nonvolatile (i.e., with soot cores) calculated for the HS plume is comparable to the concentration measured in the LS plume (that is, $\sim 6,000/\text{cm}^3$). This comparison suggests that the relative abundance of volatile and non-volatile aerosols predicted for the HS plume are reasonable.

The simulated total concentration of particles with diameters $> 7 \text{ nm}$ is about $30,000/\text{cm}^3$ at 21 sec , which is somewhat higher than the average values measured by Schumann et al. (1996) ($\sim 20,000/\text{cm}^3$). However, based on the shape of the predicted size distributions in Figure 3, detected $N_{d>7 \text{ nm}}$ values may be sensitive to the instrumental counting efficiency at small sizes, high concentrations, and short sampling times. The measurements, in short, may represent a rough lower limit to the actual abundance.

Contrail Impact on Aerosol Properties: Figure 3 illustrates the size distributions of the particles in the HS plume at 21 sec , following contrail dissipation. Several modes are apparent in the volatile sulfuric acid particle size distribution (Fig. 3a). The smallest "nucleation" mode is the result of coagulation of sub-nanometer neutral $\text{H}_2\text{SO}_4\text{-H}_2\text{O}$ clusters formed in the supersaturated acid vapor. A sec-

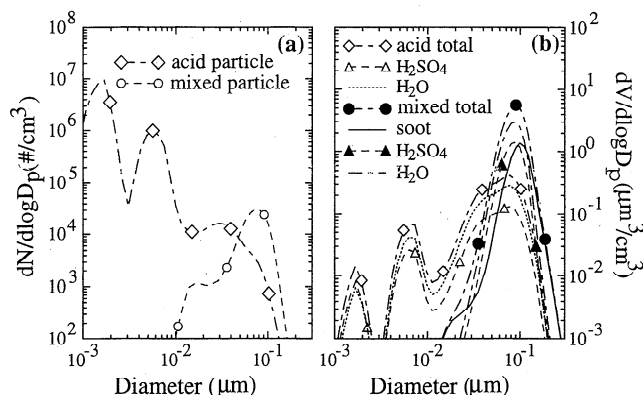


Figure 3. Size (panel a) and volume (panel b) distributions of pure acid aerosols and mixed particles at 21 sec in a high-sulfur plume for the observed ambient environmental conditions. In panel (b), the relative composition of the pure acid and mixed particles is also indicated in terms of the sulfuric acid, liquid water, and soot content.

ond peak at $\sim 5 \text{ nm}$ is the "ion" mode identified by Yu and Turco (1997). A larger "activation" mode of volatile acid particles ($\sim 30 \text{ nm}$) results from water uptake by the largest of the ion mode aerosols. Finally, an "accumulation" mode ($\sim 80 \text{ nm}$) is evident as a consequence of aerosol processing through the contrail ice phase. This selective growth process in the contrail is closely related to cloud processing of aerosols in the boundary layer (e.g., Hoppel, 1986). The various modes are seen in a different perspective through the volume size distributions of Fig. 3b.

In the case of the mixed soot-acid particles, there are two distinct size modes in Figure 3a. At $\sim 20 \text{ nm}$, a soot-dominated "condensation" mode is seen. However, a second mixed-particle "contrail" mode appears at $\sim 80 \text{ nm}$. Like the volatile "accumulation" mode aerosols, these mixed particles had been activated within the contrail and collected H_2SO_4 vapor more efficiently than equivalent unactivated particles. Considering all of the mixed particles at 21 sec , the average volume fractions of soot, H_2SO_4 , and H_2O are 23%, 25% and 52%, respectively.

The predicted mixed particle properties suggest that soot cores processed through a contrail will be transformed into effective CCN/IN for upper tropospheric clouds. Further, in the circumstance that a contrail forms in a high-sulfur plume, substantial numbers of acid particles large enough to act as CCN/IN may also be generated.

Our computed particle sizes and compositions are in accord with measurements. Hagen et al. (1996) detected significant numbers of aerosols with dry diameters of $\sim 33 \text{ nm}$ having large soluble mass fractions (many of which were fully soluble). The total particle size distribution in Figure 3a also agrees—in its general behavior—with Hagen et al.'s (1996) observed type II size distribution—i.e., a descending Junge-like distribution between $0.01 \mu\text{m}$ to $0.04 \mu\text{m}$, followed by a log-normal peak between 0.1 and $0.2 \mu\text{m}$. There are as yet no size distribution measurements capable of resolving the peaks predicted at very small diameters. However, simulations in which contrails are absent (Fig. 4) seem to be consistent with Hagen et al.'s observed type I size distribution, in which the number of particles decreases Junge-like across the size spectrum between $\sim 0.01\text{--}0.1 \mu\text{m}$ (consider the summed particle size distribution in Fig. 4a, for example). Nevertheless, significant remaining differences in the detailed structure of the size distribution are likely to be related to variations in the conditions of aerosol evolution and observation (aircraft characteristics, ambient temperature and humidity, mixing processes, plume age, etc.).

To investigate the influence of contrail formation on the properties of the aircraft particulates, the high-sulfur case illustrated in Figure 3 was rerun assuming an ambient temperature of $-50 \text{ }^\circ\text{C}$ (the threshold temperature required to create a contrail with other conditions fixed). The results, shown in Figure 4 at 21 sec , contrast sharply with those in Figure 3. The mean size of the mixed particles ($\sim 40 \text{ nm}$; Fig. 4a) is much smaller than that of the particles processed in the contrail ($\sim 80 \text{ nm}$; Fig. 3a). Likewise, the aerosol volume distribution (Fig. 4b) shows that only a few percent of the mixed particle mass is volatile. Further, compared to the situation with a contrail present, the number of pure acid particles having diameters greater than 20 nm is much lower, and the number of nanometer-sized acid particles is much

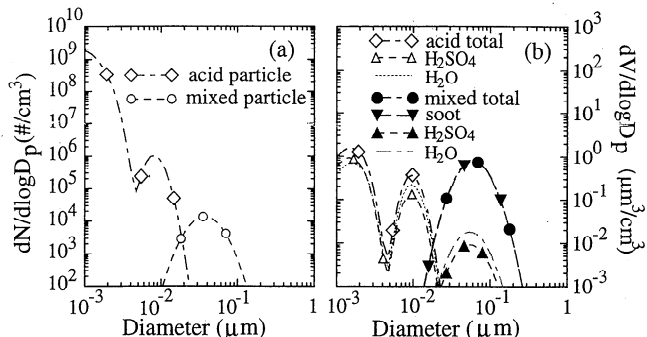


Figure 4. Size and volume distributions as in Figure 3, except that a warmer ambient temperature, $T_a = -50 \text{ }^\circ\text{C}$, has been assumed. A contrail is not formed in this case.

higher; in the latter case, the absence of ice scavenging is obviously crucial. These results lead us to conclude that contrail formation dominates the generation of CCN/IN in the aircraft wake, and that this source of cloud nuclei is amplified with higher sulfur emissions.

Summary and Discussion

We have applied a detailed aerosol microphysics model to simulate the effects of fuel sulfur content on aircraft plumes, and to perform sensitivity tests identifying key processes. Here, we focus on the high-sulfur plume data from a recent field experiment (Schumann et al., 1996). Our calculations indicate that: (1) Based on experimental data (e.g., DeMott, 1990), nearly all soot particles will be activated since the water vapor supersaturation reaches 25%; accordingly, any variation in the observed properties of plume aerosols is unlikely to be associated primarily with variations in the soot activation fraction. (2) The enhanced growth rate of small acid aerosols owing to ion-charge effects leads to a substantial number of large volatile particles capable of being activated and influencing the optical thickness of the early contrail; only a relatively few of these particles remain water-activated long enough to freeze homogeneously. (3) The predicted concentration of particles greater than 18 nm in diameter, $N_{(>18 \text{ nm})} \sim 10,000/\text{cm}^3$, is consistent with measurements, while the simulations indicate that about half of these particles are volatile; for particles larger than 7 nm, the predictions are somewhat higher than observations (however, the ability to measure accurately such high concentrations of fine particles during plume transit may be questioned). (4) Contrail formation seems to be important in creating CCN/IN in the exhaust stream, inasmuch as exhaust particles that evolve through a contrail have considerably greater soluble mass fractions and are much larger in size; this is especially true for exhaust streams that contain high amounts of sulfur. (5) The simulated size distributions of the exhaust particles with and without contrail formation show two distinct types of size dispersion, which are similar in overall characteristics to those seen in the wakes of commercial aircraft. (6) Our detailed predictions reveal up to a half-dozen size modes in contrail-processed aerosols, each of which has an identifiable physical/chemical origin.

Although our simulations agree in many respects with observations, the detailed properties of the plume aerosols and contrails depend on a variety of parameters, many of which remain uncertain. Additional sensitivity studies will be carried out to define more precisely the roles of ions, soot, and fuel sulfur content in the formation, evolution, microphysics, and optics of contrails. Among the parameters to be considered are the fraction of fuel sulfur oxidized to S(VI), initial chemion concentrations, the rate of homogeneous/heterogeneous freezing of supercooled solutions, the efficiency of SO₂ heterogeneous oxidation, soot emission indices, the effects of other condensable gases such as HNO₃, and ambient temperature and humidity variations. The distinctive particle size distributions and compositions predicted here can also be tested through in situ sampling, leading to further refinements in our understanding of aircraft particulates and their effects.

Acknowledgment. This work has been supported by NASA under grants NAGW-3671 and NAG5-2723, and the National Science Foundation under grants ATM-92-16646 and ATM-96-18425. F. Y. is also supported by a UCLA Global Change Consortium Fellowship.

References

- Appleman H., The Formation of Exhaust Condensation Trails by Jet Aircraft, *Bulletin American Meteorol. Society*, **34**, 14-20, 1953.
- Brown, R. C., R. C. Miake-Lye, M. R. Anderson, C. E. Kolb and T. J. Resch, Aerosol dynamics in near-field aircraft plumes, *J. Geophys. Res.*, **101**, 22,939-22,953 1996a.
- Brown, R. C., M. R. Anderson, R. C. Miake-Lye, C. E. Kolb, A. A. Sorokin and Y. Y. Buriko, Aircraft exhaust sulfur emissions, *Geophys. Res. Lett.*, **23**, 3603-3606 1996b.
- Brown, R. C., R. C. Miake-Lye, M. R. Anderson and C. E. Kolb, Aircraft sulfur emissions and the formation of visible contrails, *Geophys. Res. Lett.*, **24**, 385-388 1997.
- Calcote, H. F., Non-equilibrium ionization in flames, Proc. Ions in Flames and Rocket Exhaust Conference, Palm Springs, California, October 10-12 1962.
- DeMott, P. J., Exploratory studies of condensation and ice nucleation by soot aerosols, *J. Appl. Meteor.*, **29**, 1072-1079, 1990.
- DeMott, P. J., and D. C. Rogers, Freezing nucleation rates of dilute solution droplets measured between -30° and -40°C in laboratory simulations of natural clouds, *J. Atmos. Sci.*, **47**, 1056-1064, 1990.
- Frenzel, A., and F. Arnold, "Sulfuric acid cluster ion formation by jet engines: Implications for sulfuric acid formation and nucleation," DLR-Mitt, 94-06, DLR, D-51140 Köln, pp. 106-112, 1994.
- Friedl, R. R., Editor, *Atmospheric Effects of Subsonic Aircraft: Interim Assessment Report of the Advanced Subsonic Technology Program*, NASA Ref. Publ., 1400, 1997.
- Gierens, K.; Schumann, U., Colors of contrails from fuels with different sulfur contents, *J. Geophys. Res.*, **101**, 16731-6, 1996.
- Hagen D. E., P. D. Whitefield and H. Schlager, Particulate emissions in the exhaust plume from commercial jet aircraft under cruise conditions, *J. Geophys. Res.*, **101**, 19551-19557, 1996.
- Hoppel, W. A., G. M. Frick and R. E. Larson, Effect of nonprecipitating clouds on the aerosol size distribution in the marine boundary layer, *Geophys. Res. Lett.*, **13**, 125-128, 1986.
- Jacobson, M. Z., and R. P. Turco, Simulating condensational growth, evaporation and coagulation of aerosols using a combined moving and stationary size grid, *Aerosol Sci. Tech.*, **22**, 73-92, 1995.
- Jacobson, M. Z., A. Tabazadeh and R. P. Turco, Simulating equilibrium with-in aerosols and nonequilibrium between gases and aerosols, *J. Geophys. Res.*, **101**, 9079-9091, 1996.
- Kärcher, B., Aircraft-generated aerosols and visible contrails, *Geophys. Res. Lett.*, **23**, 1933-1936, 1996.
- Kärcher, B., Th. Peter and R. Ottmann, Contrail formation: Homogeneous nucleation of H₂SO₄-H₂O droplets, *Geophys. Res. Lett.*, **22**, 1501-1504, 1995.
- Keil, D. G., R. J. Gill, D. B. Olson and H. F. Calcote, Ion concentration in premixed acetylene-oxygen flames near the soot threshold, In *The Chemistry of Combustion Processes*, T. M. Sloane, Ed., American Chemical Society, Washington, D.C., 1983.
- Schumann, U., On the effect of emissions from aircraft engines on the state of the atmosphere, *Ann. Geophysicae*, **12**, 365-384, 1994.
- Schumann, U., et al., In situ observations of particles in jet aircraft exhausts and contrails for different sulfur containing fuels, *J. Geophys. Res.*, **101**, 6853-6869, 1996.
- Turco, R. P., and F. Yu, Aerosol invariance in expanding coagulating plumes, *Geophys. Res. Lett.*, **24**, 1223-1226, 1997.
- Turco, R. P., P. Hamill, O. B. Toon, R. C. Whitten and C. S. Kiang, A one-dimensional model describing aerosol formation and evolution in the stratosphere: Part I. Physical processes and mathematical analogs, *J. Atmos. Sci.*, **36**, 699-717, 1979.
- WMO, *Scientific Assessment of Ozone Depletion: 1994*, World Meteorological Organization Global Ozone Research and Monitoring Project Report No. 37, 1995.
- Yu, F., and R. P. Turco, The role of ions in the formation and evolution of particles in aircraft plumes, *Geophys. Res. Lett.*, **24**, 1927-1930, 1997.
- Zhao, J., and R. P. Turco, Nucleation simulations in the wake of a jet aircraft in stratospheric flight, *J. Aerosol Sci.*, **26**, 779-795, 1995.

F. Yu and R. P. Turco, Department of Atmospheric Sciences, University of California, Los Angeles, CA 90095-1565 (e-mail: yfq@atmos.ucla.edu).

(Received September 19, 1997; Revised November 25, 1997; Accepted December 16, 1997.)